ACS Macro Letters

Letter

pubs.acs.org/macroletters

Method to Probe Glass Transition Temperatures of Polymer Thin Films

Bolin Li,[†] Xiaolin Lu,*[,†] Yonghao Ma,[†] Xiaofeng Han,[†] and Zhan Chen*[,‡]

[†]State Key Laboratory of Bioelectronics, School of Biological Science and Medical Engineering, Southeast University, Nanjing, 210096, China

[‡]Department of Chemistry, University of Michigan, 930 North University Avenue, Ann Arbor, Michigan 48109, United States

Supporting Information

ABSTRACT: A new methodology was developed to probe glass transition temperatures (T_gs) of polymer thin films supported on gold (Au) substrates and confined between two solid (silica and silver) surfaces based on the surface plasmon polariton (SFPP) signals generated by sum frequency generation (SFG) spectroscopy. The measured T_gs for polymer (poly(methyl methacrylate), poly(benzyl methacrylate) and poly(ethyl methacrylate)) thin films supported on Au substrates showed similar thickness-dependent trend, that is, the T_g decreased as the thin film thickness decreased due to the free surface effect. However, the measured T_g of the (poly(methyl methacrylate)) thin films confined between two solid surfaces increased significantly with respect to the bulk value, indicating the strong interfacial effect when the free surface was replaced by a buried interface. This method to measure the T_g can be applied to study different polymer thin films supported on metal surfaces or confined between two solid surfaces with different surface chemistries. More importantly, SFG has the unique selectivity and sensitivity to study surfaces and interfaces, providing the feasibility to develop SFG into a powerful tool to detect surface, interfacial, and bulk T_gs of a polymer thin film simultaneously in the future.

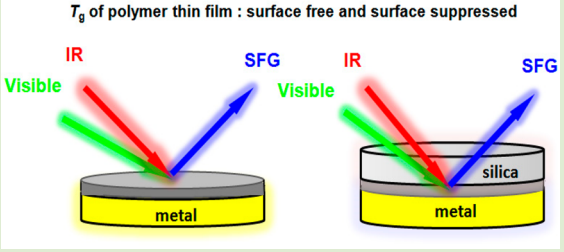

Over the last decades, thermal behaviors of polymer thin films have been extensively studied due to wide applications in materials science.[1] A fundamental question to be answered is whether and how the glass transition and the related dynamic behavior of a polymer thin film deviate from its bulk. Many techniques suitable for thin film studies including ellipsometry,[2−6] brillouin light scattering,[7] neutron reflectivity,[8] fluorescence spectroscopy,[9,10] near-edge X-ray absorption fine structure,[11] gold nanoparticle embedding,[12] X-ray reflectivity,[13] and scanning viscoelasticity microscopy[14] have been applied to investigate the glass transition temperatures (T_gs) of polymer thin films or the structural relaxation dynamics near surfaces or interfaces. It has been shown the measured polymer film T_g can be different from the bulk, and several factors were used to interpret such difference. One factor is the effect of a free surface, which has a high mobile layer and tends to decrease the T_g.[2,3,9,12,15,16] The other factor is the effect of an attractive interface at the supported substrate, which tends to decelerate the relaxation dynamics or increase the T_g.[3,13,17] Besides, chain confinement and finite size effects also play important roles. Regarding the former, the chain conformation[18,19] and chain motion mode[20] in a confined environment can be different and may lead to different dynamic behaviors. Regarding the latter, the T_g deviation as a function of film thickness may follow certain scaling relations associated with the spatial inhomogeneity of the polymer thin film,[2,3,21] as the film thickness decreases to a critical value. As a nonlinear optical technique, sum frequency generation (SFG) spectroscopy has also been used to probe T_gs or dynamic behaviors of polymer surfaces and interfaces. Examples include polypropylene,[22] poly(vinyl alcohol),[23] combed alkyl side chain polyacrylates,[24] poly(methyl methacrylate) (PMMA),[25] and polystyrene.[26,27] Owing to the surface and interface sensitivity,[28] the temperature-dependent nonlinear susceptibility ($\chi^{(2)}$) from polymer functional groups probed by SFG can be correlated to the structural dynamics occurring at a polymer surface or interface at the molecular level and in situ. Different from the above studies, in this letter, using SFG spectroscopy as a characterization technique and metal as the substrate to generate surface plasmon polariton (SFPP) signal, we developed a new methodology to measure T_gs of polymer thin films supported on metal substrates and confined between two solid (silica and metal) surfaces.

As a second-order nonlinear optical technique, SFG is forbidden for materials with inversion symmetry, but allowed at surfaces or interfaces where inversion symmetry is broken. For a thin layer of molecules on a metal substrate, the molecular vibrational transition can be probed by SFG when the frequency of the input infrared beam is tuned to the resonant frequency of the corresponding molecular vibrational mode.

Received: March 13, 2015
Accepted: April 22, 2015
Published: April 23, 2015

DOI: 10.1021/acsmacrolett.5b00185
ACS Macro Lett. 2015, 4, 548−551

Simultaneously, a strong surface plasmon polariton (SFPP) signal can be generated by the input visible beam due to the optical nonlinearity of the metal surface.[29] In view of this, we deposited PMMA (Sigma-Aldrich, M_w = 120000) thin films (Figure S1) on Au substrates by spin coating. After annealing the films at 120 °C for 4 h, we collected SFG signals from PMMA films on Au. Figure 1 shows the SFG *ppp* (p-polarized

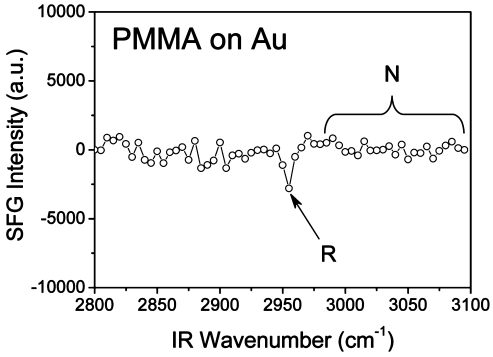

Figure 1. SFG *ppp* spectrum of a 30 nm thick PMMA thin film on Au. The molecular vibrational signals appeared as a distinct peak (denoted by "R"), while the SFPP signal appeared as the nonresonant background (denoted by "N").

output sum frequency beam, p-polarized input visible beam, and p-polarized input infrared beam) spectrum of a 30 nm thick PMMA film on Au. In this spectrum, the molecular vibrational signals appeared as a distinct resonant peak, denoted by "R" in Figure 1; while the SFPP signals appeared as the nonresonant background, denoted by "N" in Figure 1, which interfered with the resonant peaks. Here, we thermally perturbed the samples using a programmable temperature controller (Omega Engineering Series, CN 7800) and monitored the SFPP signal in the frequency range denoted by "N" in Figure 1. To be specific, the temperature was ramped at 2 K/min to a preset temperature, equilibrated for 5 min and then the SFG signal was collected (e.g., the SFG signals collected at 298 and 393 K were shown in Figure S2). In the temperature range from 295 to 400 K, the SFPP signals for a 30 nm thick PMMA sample were collected at 21 different temperatures with 5 K intervals. So were the SFPP signals for PMMA samples with thicknesses of 20, 60, and 107 nm. Figure 2A displays the average SFPP signal intensity in the frequency range "N" as a function of temperature for these samples. An abrupt change in the temperature-dependent SFG signal intensity could be observed for each sample film. To accurately determine the transition temperature, the data points before and after the abrupt change were linearly fitted and the transition temperatures were indicated by the intersection points. Clearly the transition temperature denoted by the intersection point decreased as the film thickness decreased, as shown in Figure 2B. When the film was thick enough, the transition temperature approached the bulk T_g measured by differential scanning calorimetry (DSC), indicated by an arrow in Figure 2B. This confirms that the detected transitions should be originated from the T_g transitions of PMMA thin films. To verify this methodology is widely applicable for other polymer thin films, the T_gs of poly(benzyl methacrylate) (PBMA, Sigma-Aldrich, M_w = 70000) and poly(ethyl methacrylate) (PEMA, Sigma-Aldrich, M_w = 515000) thin films on Au were also investigated. The results (see Supporting Information) demonstrated that the T_gs

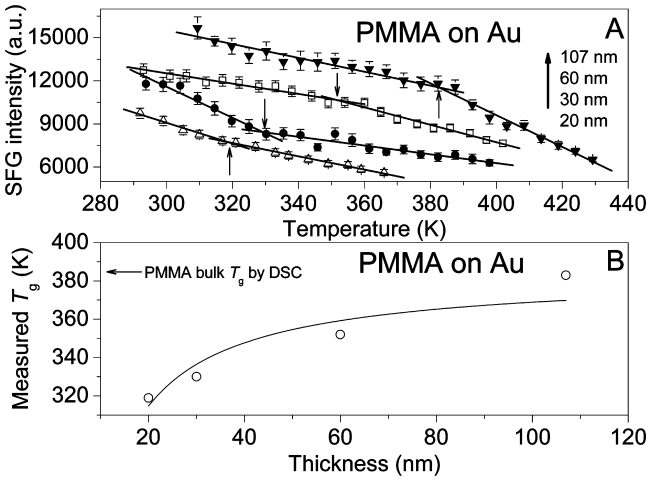

Figure 2. SFG SFPP signals as a function of temperature for PMMA thin films on Au. (A) The average SFPP intensities in the frequency range "N" as a function of temperature. Data are offset for clarity. The measured transition temperatures are indicated by arrows. (B) The deduced T_gs (open dots) from (A) as a function of film thickness. The bulk T_g measured by DSC is indicated by an arrow (see Supporting Information). The curve shows the fitting result using eq 2, which will be discussed below.

of both PBMA and PEMA thin films can be successfully determined using this method.

We believe the detected SFPP signal was generated from the Au substrate surfaces. Since there is a polymer thin film on Au, physical properties of the thin film strongly affect the SFPP signal. Upon thermal perturbation, change of the SFPP signal reflects change of the physical properties of the thin film, that is, refractive index and film thickness, which are directly related to the SFG signal from the metal surface via the optical reflection and refraction. This is the intrinsic reason why the SFPP signal can be used to probe the thermal transition of a polymer thin film on metal. For the SFPP signal intensity, we have

$$I_{SFPP} \propto |F_{SFPP}(n_i, d)\chi_{SFPP}|^2 \quad (1)$$

where I_{SFPP} is the detected SFG SFPP signal; $F_{SFPP}(n_i,d)$ is the local field coefficient responsible for all the reflections and refractions of the input fields and output field leading to the SFPP signal; χ_{SFPP} is the second-order optical nonlinearity of the metal surface. Since $F_{SFPP}(n_i,d)$ is dependent on the film refractive index and thickness, change of these two parameters leads to change of $F_{SFPP}(n_i,d)$ and I_{SFPP}. Figure 2 (also Figure S4) demonstrated that the SFPP signal is sensitive enough for probing the thermal transitions of polymer thin films on metal.

We then studied glass transition of a polymer thin film confined between two solid (silica and metal) surfaces using a sandwiched geometry as we developed before.[30,31] The SFG experimental details of sandwiched geometry are shown in the Supporting Information. Similar to the above studies, thermal perturbation could change the physical properties of the sandwiched films and such a change can be monitored from change of the SFPP signal from the Ag surface. Figure 3A shows the SFPP signal intensity as a function of temperature for PMMA thin films confined between solid silica and Ag surfaces. For all the PMMA thin films, the SFPP signal initially remained constant at the low temperature range. Then the SFPP signal for the films with different thicknesses started to increase at different temperatures as the temperature continued to

DOI: 10.1021/acsmacrolett.5b00185
ACS Macro Lett. 2015, 4, 548−551

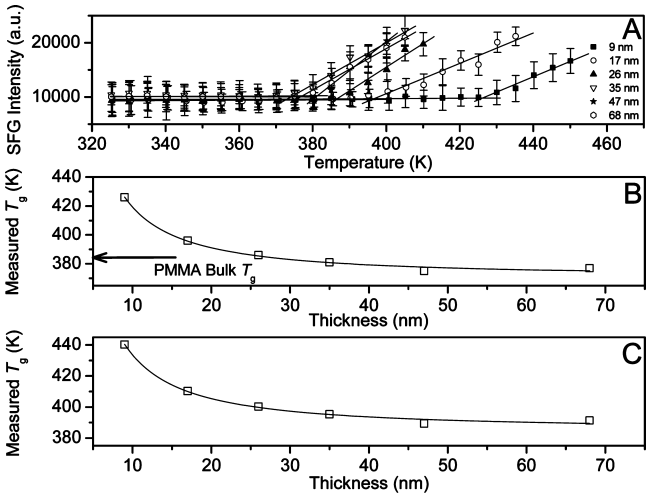

Figure 3. SFG SFPP signals as a function of temperature for the sandwiched PMMA thin films. (A) The average SFPP intensities in the frequency range "N" as a function of temperature for the PMMA films with different thicknesses. Data are offset for clarity. (B) The T_gs (open dots) from (A) as a function of the film thickness. The bulk T_g measured by DSC is indicated by an arrow. The curve shows the fitting result using eq 2. (C) The fitted curve by shifting the T_gs up by 14.3 K shown in (B).

increase. Before and after the signal increase, the data points were fitted linearly to deduce the T_gs (Figure 3A). The obtained T_g was shown as a function of film thickness in Figure 3B. Remarkably, the T_g for the sandwiched PMMA thin film decreased as the film thickness increased and finally reached a plateau. A similar relation between the measured T_g value and the film thickness has been reported by Keddie et al. for PMMA thin films on silicon with native oxide layers.[3] The higher T_g than the bulk material was attributed to the attractive interaction between PMMA and the native oxide layer. However, the measured T_gs of PMMA thin films were only several degrees higher than the bulk one in the previous report.[3] Here, in our experiment, the measured T_g is several tens of degrees higher than the bulk one when the PMMA film is very thin (Figure 3). Such a difference cannot be attributed to the effect of the attractive interaction between PMMA and the silica surface alone. Replacement of a free surface by a solid (e.g., Ag) interface must play an important role here. This demonstrates the suppression of the free surface can significantly alter the dynamic behavior of a polymer thin film on a substrate. As shown in Figure 3B, only as the film thickness decreased down to certain values (40 to 50 nm), the measured T_g started to increase. Taking into account the notion of cooperativity[32,33] and previous experimental results,[2,3,21] the finite size effect may exist for a polymer thin film confined between two solid surfaces when the polymer thin film thickness decreases down to a critical value.

Comparing the sandwiched geometry to the supported geometry, the difference is that the free PMMA surface was replaced by a PMMA/silica interface. We believe the PMMA/Au and PMMA/Ag interfaces should behave similarly. Here, it can be seen a free surface and a strongly attractive (PMMA/silica) interface induced opposite dynamic behaviors of very thin polymer films. In order to compare effects of the free surface and attractive solid interface, the scaling relations similar to what was introduced by Keddie et al.[3] were applied in both cases to fit the data shown in Figures 2A and 3A, as shown in eq 2. The fitted results are shown in Figures 2B and 3B, respectively.

$$T_g(d) = T_{g,bulk}\left[1 \pm \left(\frac{A}{d}\right)^{\delta}\right] \quad (2)$$

Here "+" was used for the sandwiched geometry and "−" was used for the supported geometry. For the sandwiched geometry, we found $T_{g,bulk}$ = 370.7 K, A = 2.0 ± 0.4 nm, and δ = 1.2 ± 0.2. For the supported geometry, we found $T_{g,bulk}$ = 385.0 K, A = 3.1 ± 2.4 nm, and δ = 0.9 ± 0.3. For the supported geometry, A should be associated with the length scale of the near-surface mobile layer leading to the T_g decrease. For the sandwiched geometry, A should be associated with the length scale describing the interfacial effect leading to the T_g increase. δ here stands for the order of magnitude of the T_g variation in terms of the film thickness. In theory, the bulk T_gs from fitting for the two films should be the same. However, the obtained bulk T_gs are different, at 370.7 and 385.0 K, respectively. This should be due to the temperature calibration issues in two experiments. For the supported geometry, the temperature was directly calibrated at the Au surface, while for the sandwiched geometry, the temperature was calibrated at the silica top surface, which is far away from the heating device compared to the polymer film (see Supporting Information). Therefore, the "real" temperature of the sandwiched polymer film should be higher than the calibrated temperature. If we shift the measured temperatures 14.3 K higher than those shown in Figure 3B, the fitted results indicate that A = 1.9 ± 0.4 and δ = 1.2 ± 0.2, and the deduced bulk T_g is 385.0 K. Figure 3C shows the shifted data and the fitted curve.

In summary, using SFG spectroscopy and metal substrates, we developed a "metal-surface-plasmon-polariton" methodology to probe dynamic behaviors of polymer thin films. The SFG SFPP signals for two sample geometries, polymer thin films directly deposited on metal substrates and polymer thin films confined between two solid surfaces (with one transparent and one metal substrate surface), could be easily detected as a function of temperature. For the supported geometry, the T_g decreased as the film thickness decreased. For the sandwiched geometry, the T_g increased as the film thickness decreased. This suggests, without a free surface, the silica−PMMA interaction can significantly influence the T_g of the PMMA thin film, evidenced by a T_g several tens of degrees higher than that of the bulk for a very thin film (9 nm). The methodology developed in this study can be used to probe polymer thin films confined between two solid surfaces in situ. It can therefore be further applied to probe dynamic behaviors of polymer thin films sandwiched between two solid surfaces with different surface chemistries. More importantly, by combining the SFG resonance signal analysis, the dynamic behavior of the entire thin film detected in this study can be used to compare to the surface and interfacial dynamic behaviors of polymer thin films, providing in-depth understanding on the molecular structures/dynamics of polymer thin film surface, interface, and bulk simultaneously.

■ ASSOCIATED CONTENT

Ⓢ Supporting Information

Chemical formulas of the polymers employed in this study, DSC experiment, SFG experimental results of the supported PBMA, PEMA thin films, SFG experimental details of sandwiched geometry, and temperature calibration experiment.

DOI: 10.1021/acsmacrolett.5b00185
ACS Macro Lett. 2015, 4, 548−551

This material is available free of charge via the Internet at http://pubs.acs.org.

AUTHOR INFORMATION

Corresponding Authors

*E-mail: lxl@seu.edu.cn. Tel.: 86-25-83791810.
*E-mail: zhanc@umich.edu.

Notes

The authors declare no competing financial interest.

ACKNOWLEDGMENTS

This study was supported by the National Natural Science Foundation of China (Grant 51173169), Scientific Research Foundation for the Returned Overseas Chinese Scholars, Ministry of Education of China. X.L. is also grateful for the Project Funded by the Priority Academic Program Development of Jiangsu Higher Education Institutions, China (PAPD).

REFERENCES

(1) Yampolskii, Y.; Pinnau, I.; Freeman, B. D. *Materials Science of Membranes for Gas and Vapor Separation*; John Wiley and Sons, Ltd.: England, 2006.
(2) Keddie, J. L.; Jones, R. A. L.; Cory, R. A. *Europhys. Lett.* **1994**, *27*, 59−64.
(3) Keddie, J. L.; Jones, R. A. L.; Cory, R. A. *Faraday Discuss.* **1994**, *98*, 219−230.
(4) Sharp, J. S.; Forrest, J. A. *Phys. Rev. Lett.* **2003**, *91*, 235701.
(5) Bäumchen, O.; McGraw, J. D.; Forrest, J. A.; Dalnoki-Veress, K. *Phys. Rev. Lett.* **2012**, *109*, 055701.
(6) Pye, J. E.; Roth, C. B. *Phys. Rev. Lett.* **2011**, *107*, 235701.
(7) Forrest, J. A.; Dalnoki-Veress, K.; Stevens, J. R.; Dutcher, J. R. *Phys. Rev. Lett.* **1996**, *77*, 2002−2005.
(8) Inoue, R.; Kawashima, K.; Matsui, K.; Nakamura, M.; Nishida, K.; Kanaya, T.; Yamada, N. L. *Phys. Rev. E* **2011**, *84*, 031802.
(9) Priestley, R. D.; Ellison, C. J.; Broadbelt, L. J.; Torkelson, J. M. *Science* **2005**, *309*, 456−459.
(10) Ellison, C. J.; Torkelson, J. M. *Nat. Mater.* **2003**, *2*, 695−700.
(11) Wallace, W. E.; Fischer, D. A.; Efimenko, K.; Wu, W. L.; Genzer, J. *Macromolecules* **2001**, *34*, 5081−5082.
(12) Fakhraai, Z.; Forrest, J. A. *Science* **2008**, *319*, 600−604.
(13) Wallace, W. E.; van Zanten, J. H.; Wu, W. L. *Phys. Rev. E* **1995**, *52*, R3329−R3332.
(14) Kajiyama, T.; Tanaka, K.; Takahara, A. *Macromolecules* **1997**, *30*, 280−285.
(15) Forrest, J. A.; Dalnoki-Veress, K. *Adv. Colloid Interface Sci.* **2001**, *94*, 167−196.
(16) Yang, Z. H.; Fujii, Y.; Lee, F. K.; Lam, C. H.; Tsui, O. K. C. *Science* **2010**, *328*, 1676−1679.
(17) van Zanten, J. H.; Wallace, W. E.; Wu, W. L. *Phys. Rev. E* **1996**, *53*, R2053−R2056.
(18) Bitsanis, I.; Hadziioannou, G. *J. Chem. Phys.* **1990**, *92*, 3827−3847.
(19) Baschnagel, J.; Binder, K. *Macromolecules* **1995**, *28*, 6808−6818.
(20) de Gennes, P. G. *Eur. Phys. J. E* **2000**, *2*, 201−205.
(21) Mattsson, J.; Forrest, J. A.; Börjesson, L. *Phys. Rev. E* **2000**, *62*, 5187−5200.
(22) Gracias, D. H.; Zhang, D.; Lianos, L.; Ibach, W.; Shen, Y. R.; Somorjai, G. A. *Chem. Phys.* **1999**, *245*, 277−284.
(23) Zhang, C.; Hong, S.-C.; Ji, N.; Wang, Y. P.; Wei, K. H.; Shen, Y. R. *Macromolecules* **2003**, *36*, 3303−3306.
(24) Gautam, K. S.; Dhinojwala, A. *Phys. Rev. Lett.* **2002**, *88*, 145501.
(25) Li, Q. F.; Hua, R.; Cheah, I. J.; Chou, K. C. *J. Phys. Chem. B* **2008**, *112*, 694−697.
(26) Harp, G. P.; Rangwalla, H.; Li, G. F.; Yeganeh, M. S.; Dhinojwala, A. *Macromolecules* **2006**, *39*, 7464−7466.
(27) Tsuruta, H.; Fujii, Y.; Kai, N.; Kataoka, H.; Ishizone, T.; Doi, M.; Morita, H.; Tanaka, K. *Macromolecules* **2012**, *45*, 4643−4649.
(28) Shen, Y. R. *Nature* **1989**, *337*, 519−525.
(29) Liebsch, A. *Appl. Phys. B: Laser Opt.* **1999**, *68*, 301−304.
(30) Lu, X. L.; Li, D. W.; Kristalyn, C. B.; Han, G. L.; Shephard, N.; Rhodes, S.; Xue, G.; Chen, Z. *Macromolecules* **2009**, *42*, 9052−9057.
(31) Lu, X. L.; Li, B. L.; Zhu, P. Z.; Xue, G.; Li, D. W. *Soft Matter* **2014**, *10*, 5390−5397.
(32) Adam, G.; Gibbs, J. H. *J. Chem. Phys.* **1965**, *43*, 139−146.
(33) Fischer, E. W.; Donth, E.; Steffen, W. *Phys. Rev. Lett.* **1992**, *68*, 2344−2346.

DOI: 10.1021/acsmacrolett.5b00185
ACS Macro Lett. 2015, 4, 548−551